

# Spatial and Time Evolution of Non Linear Waves in Falling Liquid Films by the Harmonic Expansion Method with Predictor-Corrector Integration

Munoz-Cobo J.L., Miquel A, Berna C., Escrivá A.  
 Instituto de Ingeniería Energética,  
 Universitat Politecnica de Valencia,  
 Camino de Vera 14, Valencia 46022,  
 Spain,  
 E-mail: jlcobos@iqn.upv.es

## ABSTRACT

Falling film flows in vertical or inclined planes, and pipes, are present in the energy and chemical industry (Chemical reactors, evaporators, condensers...). The occurrence of waves in these falling films is of relevance because it enhances the heat and mass transfer in comparison with a flat film.

Perturbation theory can be applied to the Navier-Stokes (NS) equations expressing the velocity and the pressure in terms of an order formal parameter representing the smallness of the stream wise spatial derivative. Normally good results are obtained for this kind of problems solving the first order NS equations.

In the present work we use the integral approach method and we expand the velocity profile of the falling liquid in a complete orthogonal set of harmonic functions satisfying the boundary conditions of the NS problem in first order approximation of the formal expansion. The present model does not assume self-similar profile of the velocity and its convergence to the solution is good with few harmonics.

The problem is discretized by means of a uniform grid. Then the partial differential equations are integrated over the length of an arbitrary node. Proceeding in this way we have obtained a set of coupled ordinary differential equation system (ODES) for the harmonics of the flow rate and the film thickness at each grid node. The resulting coupled ODES is integrated by a semi-implicit predictor-corrector method of the Adams-Moulton type that converges, with one iteration, at each time step.

The method predicts well the experimental data on the evolution of the waves with time, the height of the waves, the wave separation, and the wave profiles for different experimental conditions. Providing a physical understanding of the non-linear wave phenomena produced in falling films.

## INTRODUCTION

The dynamics of falling films is encountered in a wide variety of industrial applications as condensers, evaporators, chemical reactors, containment refrigeration of power plants and so on [1]. In addition thin films flowing down vertical or inclined surfaces are usually unstable, and in many cases non-linear waves develop on the interfacial surface of the liquid enhancing the heat and mass transfer [2]. Numerical investigation of the full Navier-Stokes equations by direct numerical simulation (DNS) methods are difficult to perform due to the extremely small time steps and spatial meshes that

should be used, in addition to the complexity introduced by the free surface [3].

## NOMENCLATURE

$B$	[-]	Cotangent of the inclination angle
$g$	[m/s <sup>2</sup> ]	Gravity acceleration
$h$	[m]	Film thickness in the cross stream direction
$f$	[s <sup>-1</sup> ]	Forced frequency of the inlet flow perturbations.
$K_a$	[-]	Kapitza number $(L_{cap}/L_v)^2$
$L_{cap}$	[m]	Capillarity length $(\sigma/\rho g \sin \theta)^{1/2}$
$L_v$	[m]	Characteristic length $(v^2/(g \sin \theta))^{1/3}$
$p$	[N/m <sup>2</sup> ]	Pressure
$q$	[m <sup>2</sup> /s]	Flow rate
$Q_a$	[-]	Amplitude of the flow perturbation
$r$	[m <sup>3</sup> /s <sup>2</sup> ]	Momentum flow rate
$u$	[m/s]	Velocity component in the stream-wise direction
$v$	[m/s]	Velocity component in the cross-stream direction
$x$	[m]	Cartesian axis in the stream-wise direction
$y$	[m]	Cartesian axis in the cross stream direction
$z$	[m]	Cartesian axis in the span-wise direction
Special characters		
$\varepsilon$	[-]	Formal parameter of the perturbation expansion
$\theta$	[-]	Inclination angle in radians.
$\nu$	[m <sup>2</sup> /s]	Kinematic viscosity
$\sigma$	[N/m]	Surface tension
Subscripts		
$a$		Atmospheric pressure
$t$		time
$0$		Undisturbed or stationary

An intermediate level of approximation is when one uses the so called boundary layer equations, which are the NS equations incorporating the condition that stream-wise gradients are small in comparison with cross stream variations. This condition allows to apply perturbation theory to the NS equations in the form of a systematic expansions in powers of a formal parameter  $\varepsilon$  that express the smallness of the stream-wise spatial derivative. However in these formal first order NS equations one must include the surface tension term that is formally of third order in the formal parameter  $\varepsilon$ . However as discussed by Ruyer-Quil and Manneville [2], the capillarity

term should be included because contributes to the evaluation of the pressure at order zero and cannot be neglected.

Several methods have been developed in the past to try to obtain the non-linear evolution of the waves generated on the surface of the thin falling films [2, 3, 4]. These long waves of increasing amplitude develop at the surface of thin layer films while the film flow remains laminar. The dynamics of these films is controlled by the viscosity, the surface tension and the gravity. The amplitude of these waves can change the heat and mass transfer on the surface, so condensation and heat transfer problems are affected by these waves [5].

The integral boundary layer method is used in this paper with an expansion of the stream-wise velocity in harmonic function that satisfy the boundary conditions in first order. This method developed by Aktershev and Alekseenko does not assume a self-similar profile for the velocity and has more degrees of freedom than the self-similarity approach.

The paper is organized as follows, first we formulate the model equations and we scale them conveniently. Then we integrate them over the boundary layer thickness (BL) obtaining the integral boundary layer equations (IBL). Then the velocity is expanded in harmonic functions that satisfy the boundary conditions of the problem. The resulting partial differential equations that results for the harmonic flow and the film thickness are solved by a new method explained in the paper, and finally the numerical solutions are compared with the experimental data [2], and a discussion of the results is performed.

## MODEL FORMULATION AND SCALING

The solution of the NS equations is performed in this paper in the so called boundary layer approximation incorporating the condition that the stream wise gradients are small when compared to cross stream variations. The basic NS equations must be completed with boundary conditions (BC) at the free surface and the plate bottom for plane geometry. The continuity of the stress at the boundary of the free surface adds two more equations originating from the normal and tangential stress components [1].

Perturbation theory can be applied to the NS equations expressing the velocity and the pressure in terms of an order formal parameter that shows the smallness of the stream wise spatial and time derivatives in comparison with the cross stream spatial derivative. Normally good results are obtained for this kind of problems solving the first order NS equations [4, 5].

In the present work we use the integral approach method and we expand the velocity profile of the falling liquid in a complete orthogonal set of harmonic functions satisfying the BC of the NS problem in first order approximation of the formal expansion. We work with dimensionless first order NS equations introducing the following characteristics length and time scales:

$$L_v = (v^2 / (g \sin \theta))^{1/3}, \quad T_v = (v / (g \sin \theta)^2)^{1/3} \quad (1)$$

In first order the 2D dimensionless NS equations are given by [1]:

$$\partial_t u + u \partial_x u + v \partial_y u = -\partial_x p + I + \partial_{yy} u \quad (2)$$

$$-\partial_y p - B + \partial_{yy} v = 0 \quad (3)$$

$$\partial_x u + \partial_y v = 0 \quad (4)$$

Where  $B = \cotg \theta$ . These previous equations must be completed with BC at  $y=0$  and  $h$ . The boundary conditions will be denoted by  $u|_0$  or  $u|_h$ . It is assumed the non-slip condition at the film bottom. The normal and tangential component of the balance of forces acting on the interface yields the following pair of boundary conditions:

$$p|_h - p_a + K_a \partial_{xx} h - 2 \partial_y v = 0 \quad (5)$$

$$\partial_y u|_h = 0$$

Where  $K_a$  is the non-dimensional Kapitza number. Also, defining the local instantaneous flow rate  $q$  as:

$$q(x, t) = \int_0^{h(x, t)} u(x, y, t) dy \quad (6)$$

One arrives to the following equation that expresses the mass conservation:

$$\partial_t h(x, t) + \partial_x q(x, t) = 0 \quad (7)$$

Integrating equation (3) between  $y$  and  $h$  and using the BC (5), yields:

$$p = p_a + B(h - y) + \partial_y v|_h + \partial_y v - K_a \partial_{xx} h \quad (8)$$

On account of equation (8) it is possible to compute  $\partial_x p$ , that when substituted into equation (2) yields after neglecting second order terms:

$$\partial_t u + u \partial_x u + v \partial_y u = 1 - B \partial_x h + K_a \partial_{xxx} h + \partial_{yy} u \quad (9)$$

Integrating equation (9) with respect to  $y$  between 0 and  $h(x, t)$ , gives on account of the BC:

$$\partial_t q + \partial_x r = h(1 - B \partial_x h + K_a \partial_{xxx} h) - \partial_y u|_0 \quad (10)$$

where the momentum flux  $r$  is defined as:

$$r(x, t) = \int_0^{h(x, t)} [u(x, y, t)]^2 dy \quad (11)$$

And the term  $\partial_y u|_0$  is the shear stress at the wall,  $y=0$ , in non-dimensional units.

Equations (7) and (10) describe the film flow in first order perturbation theory when the perturbations on the film surface are considered as a long wave in the sense that the ratio of the film thickness to the wave length is much smaller than unity.

## HARMONIC EXPANSION AND MODEL EQUATIONS

Next we use the harmonic expansion method developed by Aktershev and Alekseenko [4]. First we have chosen the following complete orthogonal set of harmonic  $\{f_j(\bar{y})\}_{j=1}^{\infty}$  being,  $\bar{y} = y/h$  and the harmonic functions defined as:

$$f_j(\bar{y}) = \sin(\omega_j \bar{y}), \quad \text{where, } \omega_j = (2j - 1)\pi/2 \quad (12)$$

That satisfy the first order boundary conditions of the stream-wise velocity for all the harmonics and verify the orthogonality relation:

$$\int_0^1 f_j(\bar{y}) f_m(\bar{y}) d\bar{y} = \delta_{jm} / 2 \quad (13)$$

Next we expand the stream-wise velocity in this base  $\{f_j(\bar{y})\}_{j=1}^{\infty}$ :

$$u(x, y, t) = \sum_{j=1}^{\infty} a_j(x, t) f_j(\bar{y}) \quad (14)$$

Due to the orthogonal character of the harmonic functions, it is obtained that the expansion coefficients are given by the expression:

$$a_j(x, t) = 2 \int_0^1 u(x, y, t) f_j(\bar{y}) d\bar{y} \quad (15)$$

Next we substitute in the model equations the stream-wise velocity by its expansion given by (14), and we compute first the flow rate  $q$ , and the momentum flux  $r$  that on account of (14) can be expressed as a sum of harmonics terms as follows:

$$q(x, t) = \int_0^h dy \sum_{j=1}^{\infty} a_j(x, t) f_j(\bar{y}) = \sum_{j=1}^{\infty} \frac{a_j(x, t) h(x, t)}{\omega_j} = \sum_{j=1}^{\infty} q_j \quad (16)$$

$$r(x, t) = \sum_{j=1}^{\infty} \sum_{m=1}^{\infty} a_j a_m h \int_0^1 f_j(\bar{y}) f_m(\bar{y}) d\bar{y} = \sum_{j=1}^{\infty} \frac{h a_j^2}{2} = \sum_{j=1}^{\infty} \frac{q_j^2 \omega_j^2}{2h} \quad (17)$$

The harmonic expansion of the non-dimensional shear stress on the wall is given by:

$$\partial_y u|_0 = \sum_{j=1}^{\infty} a_j \partial_y f_j|_0 = \sum_{j=1}^{\infty} \frac{a_j(x, t) \omega_j}{h} = \sum_{j=1}^{\infty} \frac{q_j \omega_j}{h^2} \quad (18)$$

Because the orthogonal set  $\{f_j(\bar{y})\}_{j=1}^{\infty}$  is complete in the  $[0, 1]$  interval we can expand in harmonics any function  $f(\bar{y})$  defined on this interval. For instance, the expansion of the Nusselt profile using equation (15) yields:

$$\bar{y} - \frac{1}{2} \bar{y}^2 = \sum_{j=1}^{\infty} \frac{2}{\omega_j^2} \sin(\omega_j \bar{y}) \quad (19)$$

Applying the operator  $\partial_{\bar{y}}|_{\bar{y}=0}$  to both sides of equation (19) it is obtained the result:

$$\sum_{j=1}^{\infty} \frac{2}{\omega_j^2} = 1 \quad (20)$$

Direct substitution of the expansions (16), (17) and (18) in equation (10), on account of eq. (20), gives the following result:

$$\sum_{j=1}^{\infty} \left\{ \partial_x q_j + \partial_x \frac{q_j^2 \omega_j^2}{2h} - \frac{2h}{\omega_j^2} (1 - B \partial_x h + K_a \partial_{xxx} h) + \frac{q_j^2 \omega_j^2}{2h} \right\} = 0 \quad (21)$$

Due to the linear independence of the harmonics it is obtained from eq. (21) the following set of partial differential equations for the evolution of the flowrate harmonics  $q_j$ :

$$\partial_x q_j + \partial_x \frac{q_j^2 \omega_j^2}{2h} = \frac{2h}{\omega_j^2} (1 - B \partial_x h + K_a \partial_{xxx} h) - \frac{q_j^2 \omega_j^2}{2h} \quad (22)$$

These equations are coupled to the evolution equation of the film thickness that on account of eq. (7) and (16) is given by:

$$\partial_t h(x, t) + \sum_{j=1}^{\infty} \partial_x q_j(x, t) = 0 \quad (23)$$

Equation (22) and (23) are the cornerstone equations of the harmonic expansion method and must be supplemented with

initial and boundary conditions for the flow rate harmonics  $q_j$  and the film thickness.

The linear stability analysis of the first order harmonic equation have been performed by Aktershev and Alekseenko [4] and will not be repeated here. However a newly developed integration of the non-linear equations and its application to different experiments will be shown in the next sections.

## INTEGRATION NUMERICAL PROCEDURE

To obtain the shape of the waves and the wave evolution under different regimes we have developed a method to integrate the set of equations (22) and (23) numerically. The calculation interval was set equal to the experimental one i.e.  $0 \leq x \leq L$  was set. An uniform grid was set with node boundaries given by  $x_i = (i-1)\Delta x$ , with  $i = 1, 2, \dots, N+1$ , the coordinates of each node were taken at the centre of the nodes and denoted by overbars i.e.  $\bar{x}_i = (i-1)\Delta x$ . So an overbar in a magnitude with sub-index  $i$ , means that the magnitude is being calculated in the centre of the  $i$ -th node located between the boundaries  $x_i, x_{i+1}$ , while a magnitude without overbar is being calculated at the boundaries. The next step is to apply to equations (22) and (23) the averaging operator over a given node:

$$\bar{g}_i = \frac{1}{\Delta x} \int_{x_i}^{x_{i+1}} g dx \quad (24)$$

Application of the operator (24) to the set of equations (22) and (23) yields:

$$\begin{aligned} \frac{d\bar{q}_{j,i}}{dt} + \frac{\omega_j^2}{2\Delta x} \left[ \frac{q_{j,i+1}^2}{h_{i+1}} - \frac{q_{j,i}^2}{h_i} \right] &= \frac{1}{\omega_j^2} \left( 2\bar{h}_i - \frac{B}{\Delta x} (h_{i+1}^2 - h_i^2) \right) + \frac{2K_a}{\Delta x \omega_j^2} \int_{x_i}^{x_{i+1}} dx \partial_{xxx} h \\ &- \frac{\omega_j^2}{2\Delta x} \int_{x_i}^{x_{i+1}} \frac{q_j}{h^2} dx, \quad j = 1, 2, \dots, NH; i = 1, 2, \dots, N \end{aligned} \quad (25)$$

And

$$\frac{d\bar{h}_i}{dt} = -\frac{1}{\Delta x} \sum_{j=1}^{NH} (q_{j,i+1} - q_{j,i}) \quad (26)$$

Being  $N$  the number of grid nodes and  $NH$  the number of harmonics used in the calculations.

Performing an integration by parts, three times, in the term that contains the third derivative in equation (23) it is obtained after some calculus that:

$$\int_{x_i}^{x_{i+1}} h \partial_{xxx} h dx = \left[ h \partial_{xx} h - \frac{1}{2} (\partial_x h)^2 \right]_{x_i}^{x_{i+1}} \quad (27)$$

The first and second derivatives that appear in equation (27) are evaluated at the boundaries of each node.

To express the magnitudes at the node boundaries in terms of the values at the node centres we assume that:

$$h_i = (\bar{h}_{i-1} + \bar{h}_i) / 2, \text{ and } q_{j,i} = (\bar{q}_{j,i-1} + \bar{q}_{j,i}) / 2 \quad (28)$$

Because the grid is uniform this is a good approach.

Proceeding in this way and substituting eq. (27) in eq. (25), it is obtained the following set of coupled ordinary differential equations (ODEs) for the evolution of the harmonic flows:

$$\begin{aligned} \frac{d\bar{q}_{j,i}}{dt} = & -\frac{\omega_j^2}{2\Delta x} \left[ \frac{q_{j,i+1}^2}{h_{i+1}} - \frac{q_{j,i}^2}{h_i} \right] + \frac{1}{\omega_j^2} \left( 2\bar{h}_i - \frac{B}{\Delta x} (h_{i+1}^2 - h_i^2) \right) \\ & + \frac{2K_a}{\Delta x \omega_j^2} \left\{ \left[ h \partial_{xx} h - \frac{1}{2} (\partial_x h)^2 \right]_{x_{i+1}} - \left[ h \partial_{xx} h - \frac{1}{2} (\partial_x h)^2 \right]_{x_i} \right\} \\ & - \frac{\omega_j^2 \bar{q}_{j,i}}{2 h_i^2}, \quad j=1,2,\dots,NH; i=1,2,\dots,N \end{aligned} \quad (29)$$

To solve the coupled ODE system formed by equations (26) and (29), we use a semi-implicit Adams-Moulton predictor corrector method of fourth order, with the prediction step based on the Adam-Bashforth algorithm [6]. If we denote this system of differential equations by:

$$\frac{d\bar{y}}{dt} = \bar{f}(\bar{y}, t) \quad (30)$$

Where the vector  $\bar{y}$  has  $(N+1) \times NH$  components

$$\bar{y} \equiv \bar{y}(\bar{h}_1, \bar{h}_2, \dots, \bar{h}_N, \bar{q}_{1,1}, \dots, \bar{q}_{1,N}, \dots, \bar{q}_{NH,1}, \dots, \bar{q}_{NH,N}) \quad (31)$$

The algorithm from time step  $n$  to time step  $(n+1)$  proceed in four steps as follows:

i) First we compute a first estimation of the solution  $\bar{y}_{n+1}^{(0)}$  at time step  $(n+1)$  using the Adam-Bashforth predictor:

$$\bar{y}_{n+1}^{(0)} = \bar{y}_n + \frac{\Delta x}{24} [55 \bar{f}_n - 59 \bar{f}_{n-1} + 37 \bar{f}_{n-2} - 9 \bar{f}_{n-3}] \quad (32)$$

ii) Second with this estimation of the solution at time step  $(n+1)$ , we obtain a first estimation of  $\bar{f}_{n+1}^{(0)}$  of the vector field at time step  $n+1$ , given by:

$$\bar{f}_{n+1}^{(0)} = \bar{f}(\bar{y}_{n+1}^{(0)}, t_{n+1}) \quad (33)$$

iii) We iterate in Adams-Moulton correction formula, as follows:

$$\bar{y}_{n+1}^{(k)} = \bar{y}_n + \frac{\Delta x}{24} [9 \bar{f}(\bar{y}_{n+1}^{(k-1)}, t_{n+1}) + 19 \bar{f}_n - 5 \bar{f}_{n-1} + \bar{f}_{n-2}] \quad (34)$$

Where  $k$  denotes the  $k$ -th iteration.

iv) The iterations end when

$$\frac{\|\bar{y}_{n+1}^{(k)} - \bar{y}_{n+1}^{(k-1)}\|}{\|\bar{y}_{n+1}^{(k)}\|} < \varepsilon \quad (35)$$

Normally one iteration at each time step and only three harmonics is enough to obtain a good solution for this kind of problems. So that, in the calculations showed in the next section we have fixed the number of iterations to only one and the number of harmonics to three to speed up the calculations. Calculations were performed with a bigger number of harmonics and iterations to see the degree of improvement achieved when comparing with the experimental data under different regimes and boundary conditions.

A question to be explained is how to compute the initial conditions for the harmonic flow rates  $q_{j,0}$ . In this case we use expression (16), and we compute the expansion coefficients using expression (15), with the Nusselt profile at steady state, this calculation yields:

$$q_{j,0} = \frac{a_{j,0} h}{\omega_j} = \frac{6 \bar{u}_0 h_0}{\omega_j^4} = \frac{6}{\omega_j^4} q_0 \quad (36)$$

## COMPARISON WITH EXPERIMENTAL DATA AND ANALYSIS OF RESULTS

In this section first we explain some experiments performed by Liu and Gollub [2] on the development and interaction of solitary waves on film flows in inclined planes, and the predictions obtained with the harmonic method when using the integration algorithm developed in this paper. The purpose is to investigate how the grid size, the number of harmonics, the boundary conditions, the excitation frequency and other parameters influence the solution. As it is well known natural (unforced waves) due to small perturbation in the ambient are selectively amplified above the Reynolds critical number  $Re_c = 1.25 B$ . However as discussed by Liu and Gollub [2] saturated periodic waves do not appear without forcing. In this last case the non-linear development of these forced periodic waves is strongly affected by the perturbation frequency that in some of the experiments was achieved by modulating the flow rate at the flow entrance in the inclined plane according to the expression:

$$q(0, t) = q_0 (1 + Q_{pa} \sin(2\pi f t)) \quad (37)$$

Different grid sizes were used for the simulation, it was observed that when grid was refined better predictions were obtained for the secondary small waves. Figure 1 displays the simulation results obtained for the case with  $f = 1.5 \text{ Hz}$ ,  $Re = 19.33$ ,  $\sigma/\rho = 5.88 \times 10^{-5} \text{ N m}^2/\text{kg}$ , and  $\nu = 6.28 \times 10^{-6} \text{ m}^2/\text{s}$ ,  $\theta = 6.4^\circ$ , in this case we use 3 harmonic, and a coarse spatial grid in non-dimensional units of  $\Delta x = 4$ .

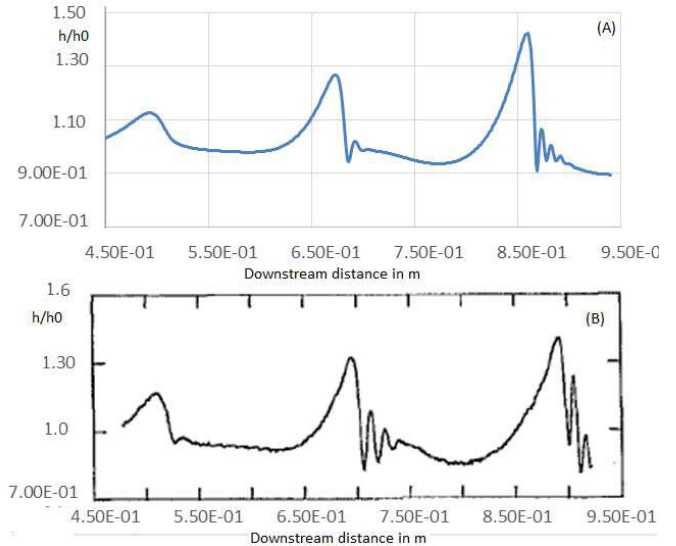


**Figure 1** Simulated (A), and Experimental results (B) for solitary waves forced at  $f=1.5 \text{ Hz}$ ,  $Re=19.33$ , Experiments from ref [2]

Because the characteristic length was  $L_v = 0.3304\text{mm}$ , this means that the grid size used to obtain figure 1 when expressed in dimensional units was  $\Delta x = 1.32\text{mm}$ . It is observed that non-linear waves of increasing amplitude are generated. These waves increase their amplitude until they reach a relative value about  $h/h_0 = 1.50$  as displayed in figure 2.

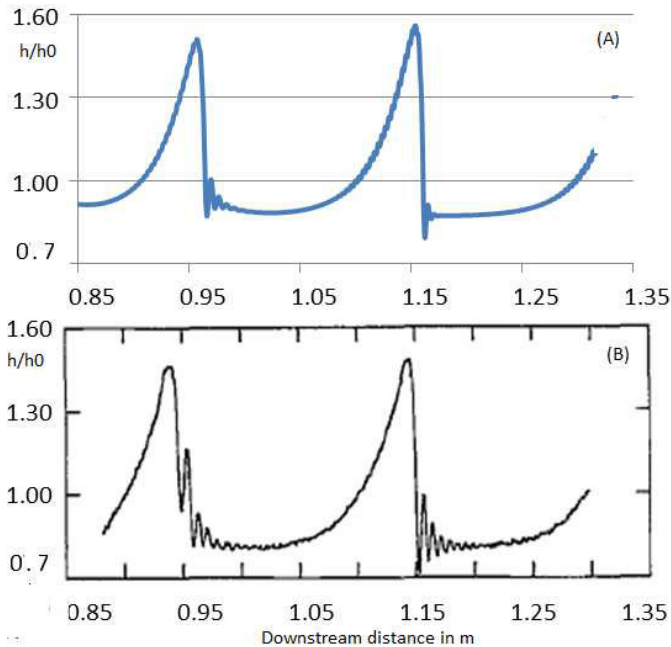


**Figure 2** Simulated (A), and Experimental results (B) for solitary waves forced at  $f=1.5\text{ Hz}$ ,  $Re=19.33$ , Experiments from ref [2]

To simulate the case with a forcing frequency of  $f = 3\text{Hz}$ , we use a finer grid with  $\Delta x = 2$  in non-dimensional units. In this case the prediction of the secondary waves was better than in the previous case, but if the size of the grid used to obtain the numerical solution increases the prediction of the secondary waves is worse as in the previous case. It is observed that when the frequency becomes larger, the primary wave fronts are closer and the waves interact significantly due to the overlapping of the wave-front of each wave with the tail of the preceding wave as noticed in figure 3.

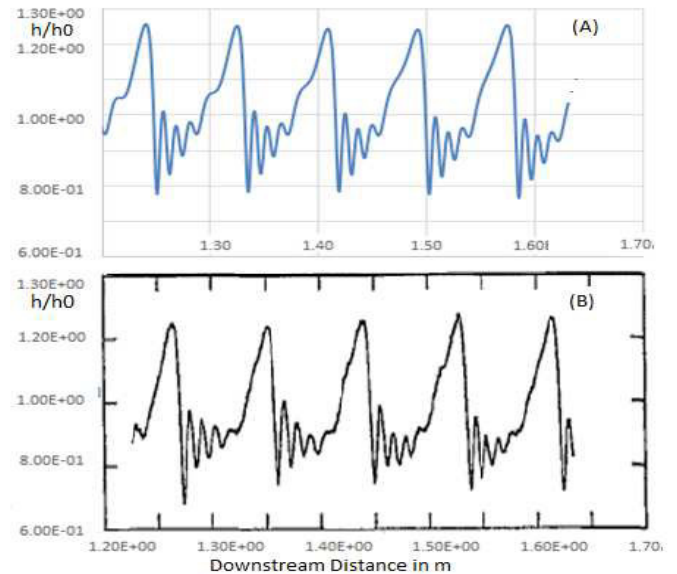


**Figure 3** Simulated (A), and Experimental results (B) for solitary waves forced at  $f=3\text{Hz}$ ,  $Re=19.33$ , Experiments from ref [2]

As the frequency increases the interaction between successive waves become more pronounced and there is an overlapping of the front of each wave with the tail of the preceding wave this produces a multi-peaked wave, because the successive waves cannot be clearly separated as displayed in figure 4. In this case the prediction is not as good as in the rest of the cases but the model captures very well the formation of the multi-peaked waves and the shape of these waves, that it is the same one that appears in the experiments as displayed in figure 4. However we must notice that the multi-peaked waves of the 4.5 Hz case appear in the experiments displaced 0.12 m downstream distance as compared with the simulation.

When we consider the length, amplitude, and shape of the waves that are obtained sufficiently far downstream from the inlet, it is obtained that the agreement with the experimental data is very good as observed in figure 5.

Therefore in the multi-peaked regime the non-linear evolution of thin films is more complex and as discussed by Ruyer-Quil and Manneville [7], three regions can be identified, corresponding to the initial exponential growth of the wave amplitude, the formation of the multi-peaked waves displayed in figure (4), and the final wave-train modulation.

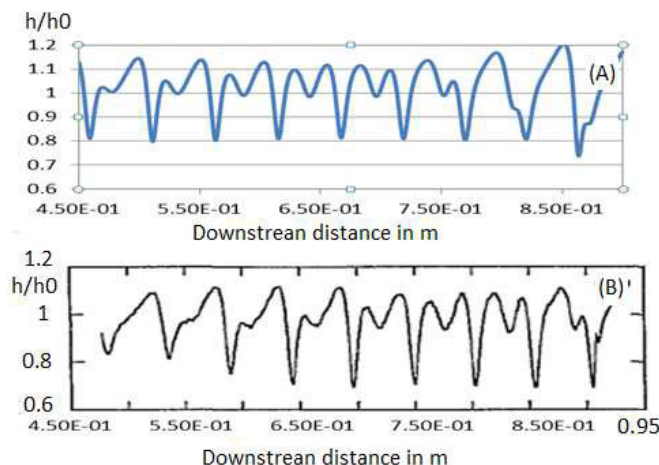


**Figure 4** Simulated (A), and Experimental results (B) for solitary waves forced at  $f=4.5$  Hz,  $Re=19.33$ , Experiments from ref [2]

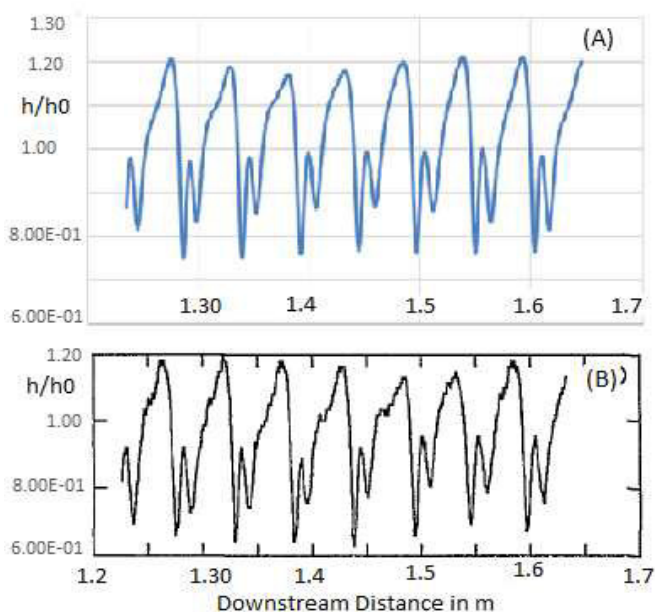


**Figure 5** Simulated (A), and Experimental results (B) for solitary waves forced at  $f=4.5$  Hz,  $Re=19.33$ , in glycerine-water experiments from ref [2]

## CONCLUSION

In this paper we have used a method based on an integral boundary layer (IBL) approach of the Navier-Stokes equations. Then we have performed an expansion of the velocity profile of the falling liquid in a complete orthogonal set of harmonic function satisfying the problem boundary conditions. We must remark that we have used a first order approximation for the Navier-Stokes equations and we have obtained good predictions of the experimental results, of Liu and Gollub [2], as displayed in figures 1,2,3,4, and 5 of this paper. The present model does not assume self-similar profile of the velocity and

its convergence to the solution is good with few harmonics, only three harmonics were used to obtain the solution for the cases of figures 1 to 5. Also we notice that the solution improved when the grid was refined, figures (1), and (2) where computed with a coarser grid than figures (3), (4) and (5) that were computed with a finer grid. In this way to have good predictions of the small subsidiary waves one must use a grid equal or smaller than 2 in non-dimensional units, but if we want a qualitative numerical solution we can use a wider grid. For this particular case one non-dimensional unit is equivalent to 0.33mm.

The numerical method developed in this paper consist in the following steps, first the problem is discretized by means of a uniform grid. Then the partial differential equations are integrated over the length of an arbitrary node. Proceeding in this way we have obtained a set of coupled ordinary differential equation system (ODES) for the harmonics of the flow rate and the film thickness at each grid node. The resulting coupled ODES is then integrated by a semi-implicit predictor-corrector method of the Adams-Moulton type that converges, with one iteration, at each time step.

The previous method predicts well the experimental data on the evolution of the waves with time, the height of the waves, the wave separation, and the wave profiles for different experimental conditions. The method also provide a good prediction of the interacting waves when the frequency increases, in particular the method reproduce the complex multi-peaked wave evolution as displayed in figure 5, where not only the peaks are reproduced, but also the frequency of these peaks. Providing a physical understanding of these phenomena.

## ACKNOWLEDGMENTS

The authors of this paper are indebted to the support received from the I+D project MODEXFLAT, ENE2013-48565-C2-1-P of the Spanish Government.

## REFERENCES

- [1] Ruyer-Quil C., Manneville P., Modeling film flows down inclined planes, *European Physical Journal B*, 6, 1998, pp 277-292.
- [2] Liu J., and Gollub J.P., Solitary wave dynamics of film flows, *Physics of Fluids*, Vol 6, No 5, 1994, pp 1702-1712.
- [3] Ramaswamy B., Chippada S., and Joo S.W., A full scale numerical study of interfacial instabilities in thin-film flows, *Journal of Fluid Mechanics*, Vol 325, 1996, pp163-194.
- [4] Aktershev S.P., Alekseenko S.V., New model for waves in falling film. *IUTAM Symposium on Waves in fluids*, Proceedings IUTAM 8, 2013, pp 3-12.
- [5] Ding Z., and Wong T.N., Falling liquid films on a slippery substrate with Marangoni effects, *International Journal of Heat and Mass Transfer*, Vol. 90, 2015, pp. 689-701
- [6] Mynkowycz, W.J., Sparrow, E.M., Schneider G.E., Pletcher, R.H., "Handbook of Numerical Heat Transfer", edited by John Wiley and Sons ISBN 0-471-83093-3, 1988.
- [7] Ruyer-Quil C., Manneville P., Further accuracy and convergence results on the modelling of flows down inclined planes by weighted residual approximations, *Physics of Fluids*, Vol 14, 2002, pp 170-183.